Journal of New Materials for Electrochemical Systems 20, 109-113 (2017)

TiO_2-$BaTiO_3$ Composite Films as Photoanode for Dye Sensitized Solar Cell: Effect of $BaTiO_3$ Content

S.N. Sadikin, M.Y.A. Rahman* and A.A. Umar

Institute of Microengineering and Nanoelectronics (IMEN), Universiti Kebangsaan Malaysia, 43600, Bangi, Selangor, Malaysia

Received: May 02, 2017, Accepted: July 01, 2017, Available online: July 26, 2017

Abstract: *This manuscript reports the use of TiO_2-$BaTiO_3$ composite films as a photoanode in dye-sensitized solar cell (DSSC). The influence of $BaTiO_3$ content on the performance parameters of the DSSC has been investigated. The composite has been prepared on ITO glass substrate via sol-gel assisted with spin coating technique. The XRD analysis reveals that the sample is crystalline with the phase of $BaTiO_3$ and anatase TiO_2. From the FESEM observation, it was found that the pure sample contains bigger pores compared with the other samples prepared with various $BaTiO_3$ contents. The samples become more compact as the content of $BaTiO_3$ increases. The samples absorb more light in ultraviolet (UV) region than visible region. The area of absorption window varies with $BaTiO_3$ content. The device utilizing the sample with 0 and 6 wt.% $BaTiO_3$ demonstrated the lowest leak current. The device utilizing pure sample produced the highest η of 0.18%. This is due to this device utilized the sample with highest porosity, lowest leak current and charge transfer resistance, R_{ct}.*

Keywords: barium titanate, composite, DSSC, photoanode, titanium dioxide

1. INTRODUCTION

Dye-sensitized solar cells (DSSC) have been widely studied because its ability in converting light into electricity is efficient. Apart from being a low-cost solar cell, DSSC is also gaining a lot of attentions from the researchers because of its simple manufacturing procedures [1] and its concept of copying the process of photosynthesis which contributes to quite high light to power conversion efficiency [2]. Titanium dioxide, TiO_2 is well known as a popular wide band gap metal oxide semiconductor for use in DSSC as photoanode. This is because it possesses good optical and electronic properties as well as its photocatalytic activity, especially its anatase phase [3]. The large surface area of TiO_2 further assists in more amount of dye adsorption on its surface which leads to higher optical absorption. This is because higher dye adsorption on the surface of the photoanode material allows more lights to be captured, which contributes to the generation of photo-excited electrons that are transferred into the oxide as reported by Zhang et al. 2012 [4].

To enhance the performance of DSSC, various modifications have been employed such as introducing dopants and composites into the photoanode material. Neetu et al. 2016 reported that the doping of aluminum into TiO_2 photoanode improved the dye loading on the TiO_2 surface [5], while Kim et al. 2014 study showed that the doping of nitrogen into TiO_2 photoanode improved electrons injection and enhanced the electron transport [6]. In another study by Hu et al. 2013, the recombination process of electrons was depressed by introducing strontium oxide shell coating on TiO_2 and hence increased the light to electricity conversion efficiency [7]. Zhu et al. 2014 found that graphene-TiO_2 composite photoanode resulted in high energy conversion efficiency due to the increase in photocurrent density and open-circuit voltage [8]. Dong et al. 2014 proved that the silver-loaded TiO_2 composite speed up the electron transport by improving dye adsorption which leads to significant increase in the performance of DSSC [9].

The goal of this work is to investigate the effect of $BaTiO_3$ content on the properties of TiO_2 films such as morphology and optical absorption and relate those properties with the photovoltaic performance parameters of DSSC utilizing TiO_2-$BaTiO_3$ composite photoanode. The originality of the work is the use of TiO_2-$BaTiO_3$ composite films as photoanaode in DSSC. According to the author's knowledge, the use of this composite as photoanode in DSSC has yet to be reported.

*To whom correspondence should be addressed: Email: mohd.yusri@ukm.edu.my
Phone: 60389118543

2. EXPERIMENTAL

2.1. Preparation of TiO_2-$BaTiO_3$ thin films and device fabrication

The materials used in this work are titanium (IV) butoxide (97.0%), acetic acid (99.7%), barium titanate (IV) purchased from Sigma-Aldrich and absolute ethanol (99.98%). Barium titanate solution was prepared by dissolving 0.30 g of barium titanate (IV) powder into 25 ml of ethanol and sonicated for 15 minutes. Then, TiO_2 solution was prepared separately by adding 1.05 ml of titanium (IV) butoxide into 7.58 ml of ethanol. These two solutions were mixed. 0.172 ml of acetic acid was added into the mixture solution to prevent coagulation. The barium titanate solution was added into the TiO_2 solution at various compositions, namely, 2, 4, 6 and 8%, respectively. Pure TiO_2 solution without adding $BaTiO_3$ was also prepared as reference and denoted as 0% $BaTiO_3$. The whole process was carried out at 80 ^oC and under stirring. Finally, the TiO_2-$BaTiO_3$ solution was left under stirring for 10 hours at 80 ^oC. Then, the solution was deposited onto ITO substrates by using spin-coating method. To ensure that the solution is dispersed uniformly on the substrates, the spin-coating was carried out at two steps, first at 500 rpm for 5 seconds and followed by 2500 rpm for 40 seconds. The spin-coating cycle was repeated for five times for each speed with drying process at 100 ^oC for 10 minutes interval between each cycle to get sufficient thickness of the film. The prepared films were annealed at 400 ^oC for 2 hours.

0.5 mM of N719 dye solution was prepared as a sensitizer. TiO_2-$BaTiO_3$ films were immersed in the dye solution for 20 hours to ensure sufficient amount of dye was coated on the surface of the samples. A DSSC was fabricated by utilizing the TiO_2-$BaTiO_3$ films coated N719 dye as the photoanode. ITO substrate coated platinum was utilized as a counter electrode of the device. Redox electrolyte containing iodide/triiodide was injected into the active area of the device before undergoing its performance studies in dark and under illumination of light.

2.2. TiO_2-$BaTiO_3$ films characterization and performance studies

The prepared TiO_2-$BaTiO_3$ film samples were characterized by using X-ray diffractometer model Bruker D8 Advanced to study the phase structure that present in the samples. The diffraction angle, 2θ used was from 10^o to 80^o. The surface morphology was characterized by a field emission electron microscope (FESEM) model MERLIN. The purpose of this characterization was to study the surface morphology of TiO_2-$BaTiO_3$ films with various concentrations of $BaTiO_3$. The UV-Vis spectrophotometer was used to study the optical absorption of the samples with various $BaTiO_3$ contents.

The DSSC was tested in the dark and under the light illumination of 100 mW cm^{-2} to obtain the *J-V* characteristics. The illuminated area was 0.23 cm^2. The charge transport properties of the device were also studied by carrying out the electrochemical impedance spectroscopy (EIS) analysis. The bulk resistance and charge transfer resistance were obtained from the EIS spectra.

3. RESULTS AND DISCUSSION

Fig. 1 shows the XRD pattern of TiO_2-$BaTiO_3$ composite films with 8%. The pattern shows the presence of anatase phase of TiO_2 at the diffraction angle of 25.66, 30.82, 38.26, 48.38, 55.40 and 63.14º corresponding with (101), (211), (004), (200), (211), and (213) planes, respectively. While for $BaTiO_3$, the peaks present at the diffraction angle of 22.48, 31.94, 39.22, 45.50, 51.28, 56.54 and 66.46º corresponding with (100), (110), (111), (200), (210), (211) and (220), planes, respectively. The results match with the XRD peaks of $BaTiO_3$ obtained by Nayak et al. 2014 in his study of $BaTiO_3$ prepared by solid state reaction method [11].

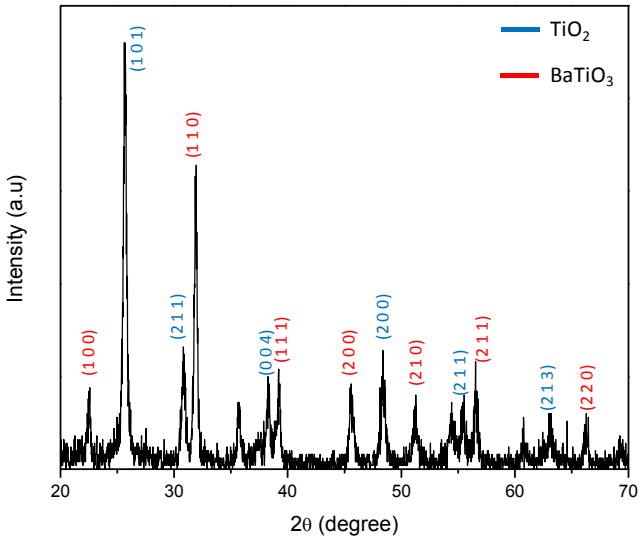

Figure 1. XRD pattern of TiO_2-$BaTiO_3$ composite films with 8% $BaTiO_3$

The FESEM images of TiO_2-$BaTiO_3$ films with various compositions of $BaTiO_3$ are shown in Fig. 2. From the figure, the pore size of the films decreases as the content of $BaTiO_3$ increases. The pure TiO_2 sample, 0% of $BaTiO_3$, possesses highest porosity followed by the sample with 2 and 4% of $BaTiO_3$. The samples with 6 and 8% of $BaTiO_3$ are more compact with less pores than the samples with lower content of $BaTiO_3$. Some of the TiO_2 nanoparticles in the samples are almost spherical and the particles are highly agglomerated as the $BaTiO_3$ content increases.

Fig. 3 shows the UV-vis spectra for TiO_2-$BaTiO_3$ thin films with various contents of $BaTiO_3$. The optical absorption of TiO_2-$BaTiO_3$ films in ultra-violet (UV) región changes with $BaTiO_3$ content. TiO_2 has the energy band gap 3.2 eV and mainly absorbs light in the UV región which is around 250-400 nm [2]. All samples absorb less light in visible región in the range 400-700 nm and infrared región which is above 700 nm. From the spectra, TiO_2 with 6% of $BaTiO_3$ content possesses the highest light absorption, followed by the samples with 8% and 4%. On the other hand, the sample with 2% $BaTiO_3$ content has the lowest light absorption.

Fig. 4 shows the dark current curves for all devices utilizing TiO_2-$BaTiO_3$ composite samples. From the figure, it can be seen that there is no increasing or decreasing trend of leak current with the variation of $BaTiO_3$ content in TiO_2. The highest leak current, was observed in the device with 2% of $BaTiO_3$ content. On the other hand, the lowest leak current and forward current were obtained in the device with 0% and 6% of $BaTiO_3$, respectively. The

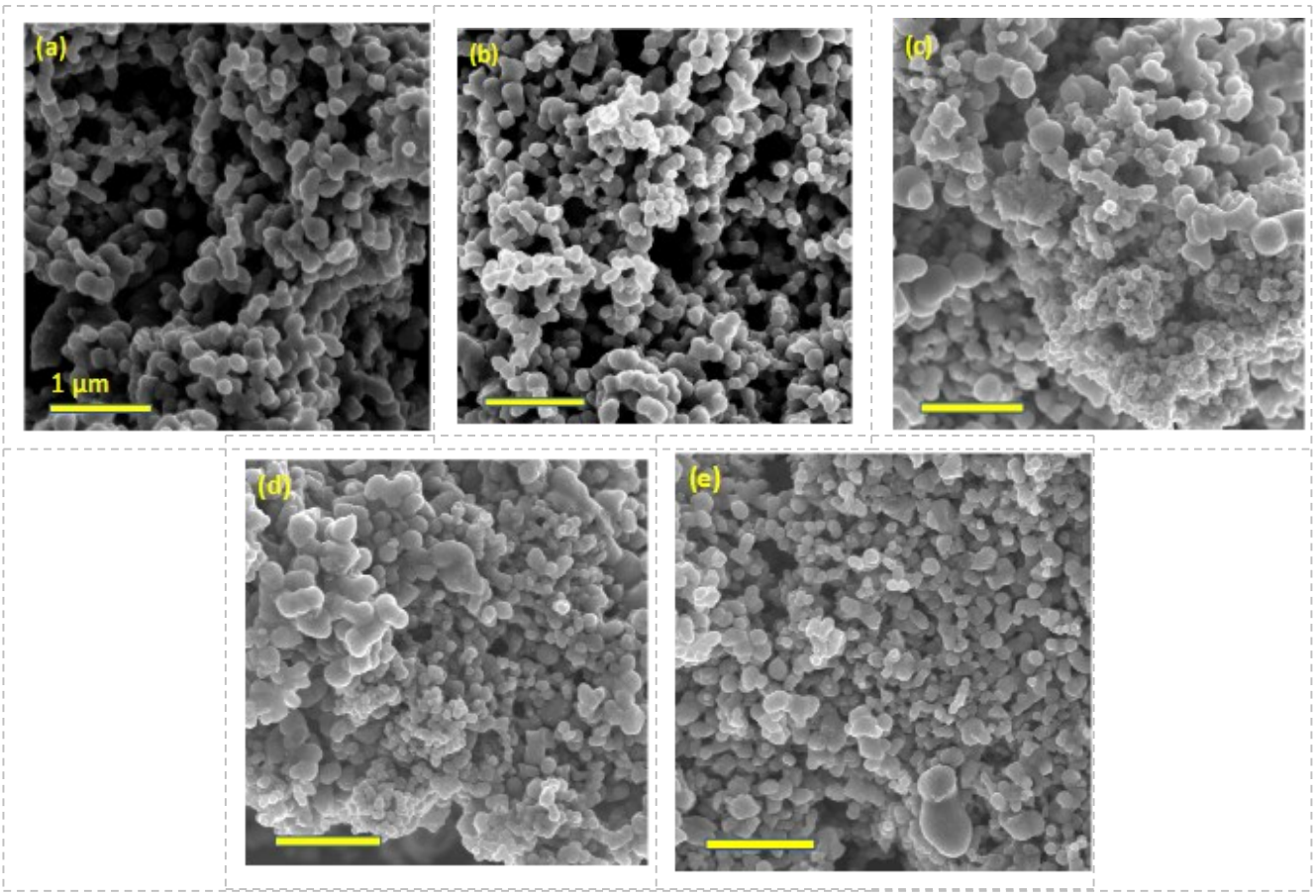

Figure 2. FESEM images of the samples with various contents of $BaTiO_3$, (a) 0 (b) 2 (c) 4 (d) 6 and (e) 8%

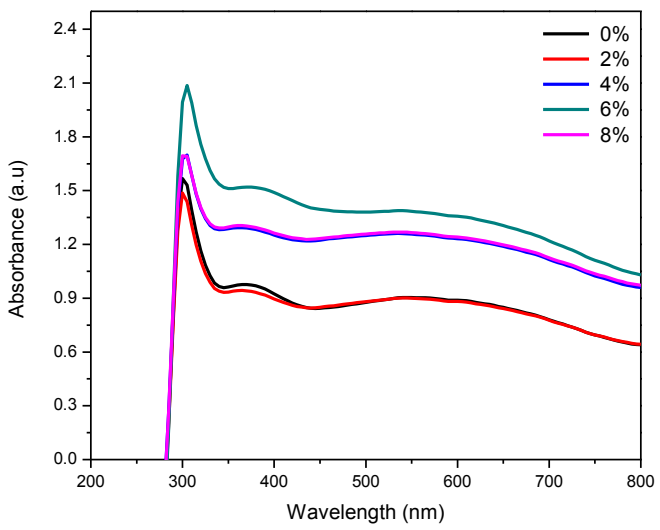

Figure 3. UV-Vis spectra of the samples with various contents of $BaTiO_3$

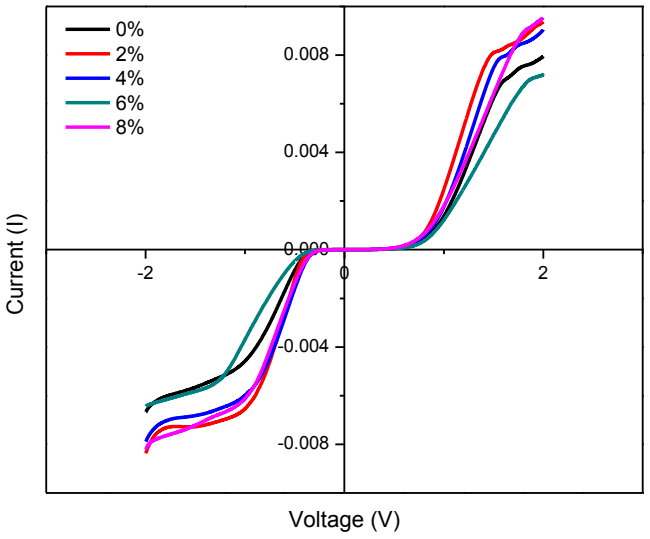

Figure 4. *I-V* curves in dark of the DSSCs utilizing TiO_2-$BaTiO_3$ photoanode with various contents of $BaTiO_3$

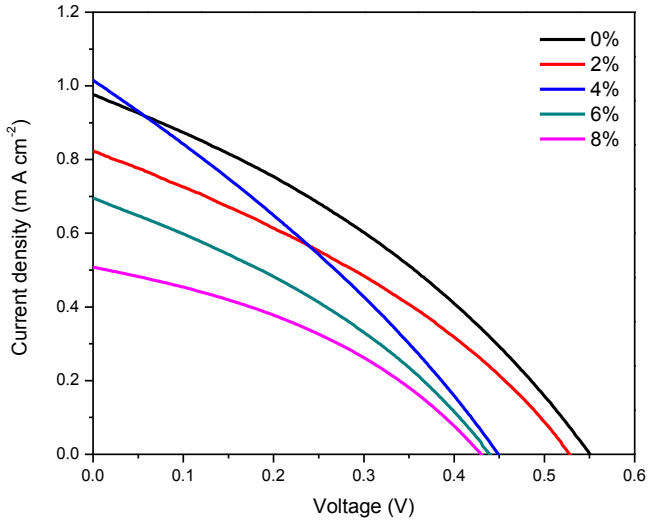

Figure 5. *J-V* curves under illumination of 100 mW cm^{-2} light of the DSSCs utilizing TiO_2-$BaTiO_3$ photoanode with various contents of $BaTiO_3$

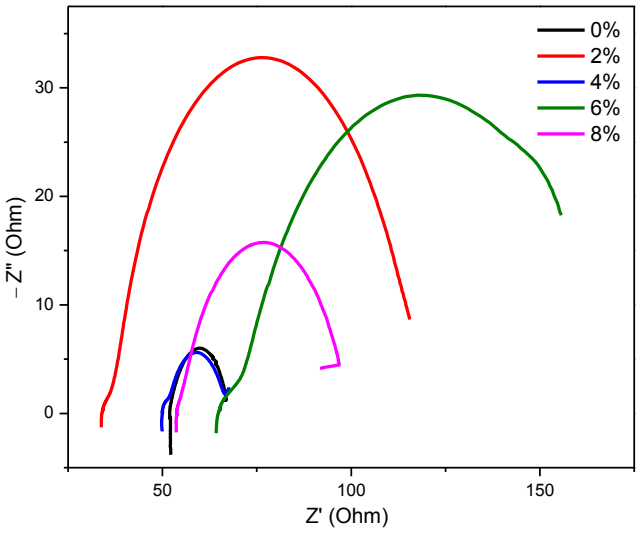

Figure 6. Nyquist plots of the DSSCs utilizing TiO_2-$BaTiO_3$ photoanode with various contents of $BaTiO_3$

dark current curves for DSSC are supposed to behave like a diode, with rectification property [12]. However, from Fig. 4, it is clear that the TiO_2-$BaTiO_3$ device does not show rectification property since the leak current curves are almost symmetry with forward current curves. The highest forward current is in the device with 2% of $BaTiO_3$.

Fig. 5 shows the *J-V* curves of the DSSC under light illumination. The slope of each curve is high which indicates the internal resistance of each device is also high. The photovoltaic parameters are also illustrated in Table 1. The device with 0% $BaTiO_3$ possesses the highest power conversión efficiency which is 0.18%. This is because of the high porosity of the sample shown in Fig. 2, allowing more dye molecules to be adsorped on the TiO_2 surface which enhances the light harvesting of the device [13]. The devices with $BaTiO_3$ have more power loss compared with the device utilizing the pure TiO_2 as the photoanode. This can be proven from the high slope of the *J-V* curves for all devices with $BaTiO_3$ which indicates the increase of internal resistance of the device. High internal resistance leads to the decrease of fill factor which in turn results in lower power conversión efficiency of the device [14].

Fig. 6 shows the Nyquist plots of the DSSC utilizing TiO_2-$BaTiO_3$ photoanode with various contents of $BaTiO_3$. The Nyquist plot consists of two semicircles. One is used to determine the bulk resistance, R_b while the second one is used to determine the charge transport resistance, R_{ct}. The bulk resistance (R_b) and charge transfer resistance (R_{ct}) are presented in Table 1. From Table 1, the R_{ct} of the device is the lowest in the pure TiO_2 photoanode, hence yielding the highest power conversión efficiency. The low R_{ct} of the device with 6% of $BaTiO_3$ is due to the high porosity of the sample, providing larger surface área which helps to improve the electron transfer [15]. While more compact photoanode surface reduces the surface área, hence restricts the electron transport in the material.

Table 1. Photovoltaic and EIS parameters of the DSSCs utilizing TiO_2-$BaTiO_3$ photoanode with various contents of $BaTiO_3$

wt. %	*J*sc (mA cm^{-2})	*V*oc (V)	*FF*	η (%)	R_b (Ohm)	R_{ct} (Ohm)
0	0.98	0.55	0.34	0.18	5.2	15
2	0.83	0.53	0.33	0.15	2.3	85
4	1.02	0.49	0.30	0.14	2.4	17
6	0.70	0.44	0.34	0.10	11.0	101
8	0.51	0.43	0.37	0.08	1.6	44

4. CONCLUSIONS

TiO_2-$BaTiO_3$ composite films has been prepared and utilized as a photoanode in dye sensitized solar cell. The influence of $BaTiO_3$ content on the morphology, optical absorption and performance of DSSC has been studied. The porosity of the TiO_2-$BaTiO_3$ films decreases with the increase of $BaTiO_3$ content. This results in lower surface area for dye loading and reduces the photocurrent in the device. The device without $BaTiO_3$ demonstrates the highest power efficiency which is 0.18% because of the fastest electron transport in the photoanode.

5. ACKNOWLEDGMENTS

This work was supported by Universiti Kebangsaan Malaysia (UKM) under research grant GUP- 2016-013.

REFERENCES

[1] H. Kim, T. Hwang, J Sol-Gel Sci. Technol., 72, 67 (2014).
[2] N.A. Ludin, A.M.A. Mahmoud, A.B. Mohamad, A.A.H. Kadhum, K. Sopian, N.S. Abdul Karim, Renew. Sustain. Energy Rev., 31, 386 (2014).
[3] S.K.M. Maarof, M. Rusop, S. Abdullah, Adv. Mater. Research,

832, 763 (2014).
[4] Q. Zhang, D. Myers, J. Lan, S.A. Jenekhe, G. Cao. Phys. Chem. Chem. Phys., 14, 14982 (2012).
[5] Neetu, I.C. Maurya, A.K. Gupta, P. Srivastava, L. Bahadur, J Solid State Electrochem., 21, 1229 (2007).
[6] S.G. Kim, M.J. Ju, I.T. Choi, W.S. Choi, H.K. Kim, Rapid Comm. Photoscience, 3, 20 (2014).
[7] Q. Hu, C. Wu, L. Cao, B. Chi, J. Pu, L. Jian, J. Power Sources, 226, 8 (2013).
[8] M. Zhu, X. Li, W. Liu, Y. Cui, Journal of Power Sources, 262, 349 (2014).
[9] H. Dong, Z. Wu, Y. Gao, A. El-Shafei, S. Ning, J. Xi, B. Jiao, Organic Electronics, 15, 2847 (2014).
[10] S. Nayak, B. Sahoo, T.P. Chaki, D. Khastgir, RSC Adv., 4, 1212 (2014).
[11] J.E. Garland, D.J. Crain, D. Roy, Electrochim. Acta, 148, 62 (2014).
[12] R. Tang, Z. Xie, S. Zhou, Y. Zhang, Z. Yuan, L. Zhang, L. Yin, ACS. Appl. Mater. Interfaces, 8, 22201 (2016).
[13] A. Mashreghi, H. Zare, J Solid State Electrochem., 20, 2693 (2016).
[14] S.H. Ahn, D.J. Kim, W.S. Chi, J.H. Kim, Adv. Funct. Mater., 24, 5037 (2014).